FLOOD-CONTROL MEASURES THAT UTILIZE NATURAL FUNCTIONS OF RIVERS

Shoji Fukuoka
Tokyo Institute of Technology, Tokyo 152, Japan

Introduction

The most important role of a river is to safely convey floodwaters downstream, protecting human life and property. Recently, people have come to demand not only functionality but also gentleness and amenity from their social capital improvement. In cities, with rivers being one of the few types of richly natural spaces, harmony with the natural environment is also demanded of flood-control projects.

It is a welcome development that authorities in charge of river works are actively promoting such projects as those involving close-to-nature river development that incorporates the needs of people and animals.

Trees and other plants in a channel play an important role in the river's ecosystem and scenic beauty, and the importance of this plant life increases in proportion to the scale of projects undertaken in a river. Conventional flood-control projects, because of their overemphasis on functionality, were unable to take full advantage of a river's natural functions. This was because (top priority being given to the protection of life and property from natural disaster) of the lack of accumulated technology for determining what kind of external-force conditions and channel conditions — balanced with the necessity of safety during flooding — would make possible the development of a close-to-nature river. This paper discusses river vegetation not only in terms of its role in river environment, but also new river technology for flood-control measure using such vegetation as a natural material in bank and levee protection.[1) 2)]

1. The mechanism by which common reed attenuates erosion on the banks of the main channel [3)]

Figure 1, which shows the effects that bank vegetation has in reducing erosion, is based on cross-sectional survey diagrams and surveys of flood channel vegetation that show to what extent the right bank of the 39-40 km section of the Tama river was eroded by flooding at that time. Severe flooding occurred here in 1974, 1979 and 1982 (August and September). While Japanese pampas grass existed in the flood channel in 1973, severe flooding in 1974 bent large amounts of this pampas grass and caused bank scouring, and by 1976 the flood channel had turned to naturally barren land. Four severe floods attacked the river during the seven years between 1976 and 1983, and although further considerable bank erosion did occur, the speed of bank erosion had been significantly reduced around the boundary with the common reed in the flood channel. In addition, the erosion has not progressed that much since 1983, a fact which demonstrates the potential of common reed as an effective material in bank protection works.

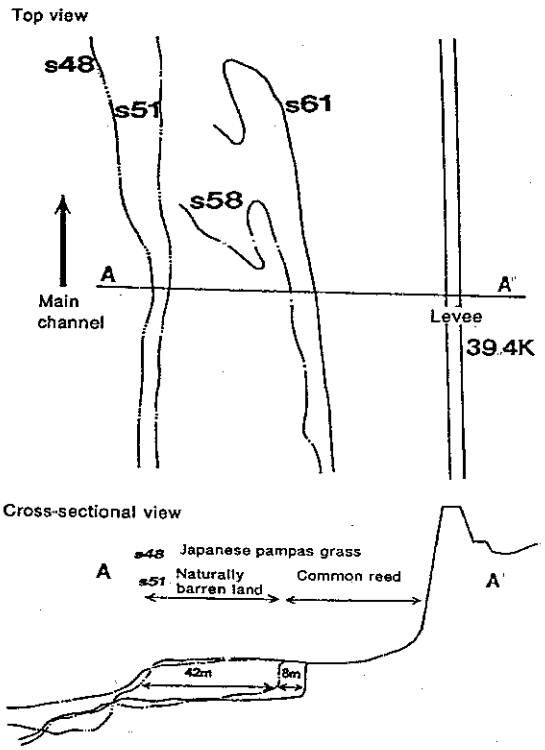

Figure 1: Changes over time in vegetation and the state of bank erosion (40 km section of Tama river)

Common reed, which grows to heights of 3 to 4 meters, possesses subterranean stems and well-developed root stalks. Growths are dense, with roughly 10 cm between stems, while subterranean stems are interconnected.

The upper layer of soil in the banks is sand, while the lower layer is gravel containing silt. When the upper layer is thin compared with the lower layer, the soil-protection effect of the reeds' root stalks (spread mat-like throughout the sand layer) increases the erosion resistance of the upper layer. The floodwaters' erosive force that acts on the banks of the main

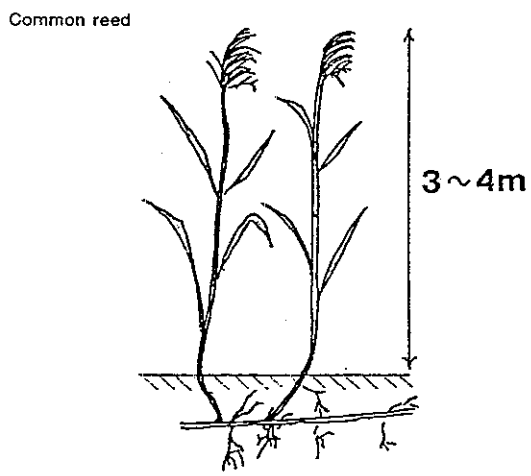

Figure 2: Common reed

channel becomes greater when the water level is between slightly higher and slightly lower than the flood channel (see Figure 3) When this happens, the silt-containing gravel layer of the lower layer, which has relatively low resistance, is eroded, leaving only upper layer containing the reed roots protruding out

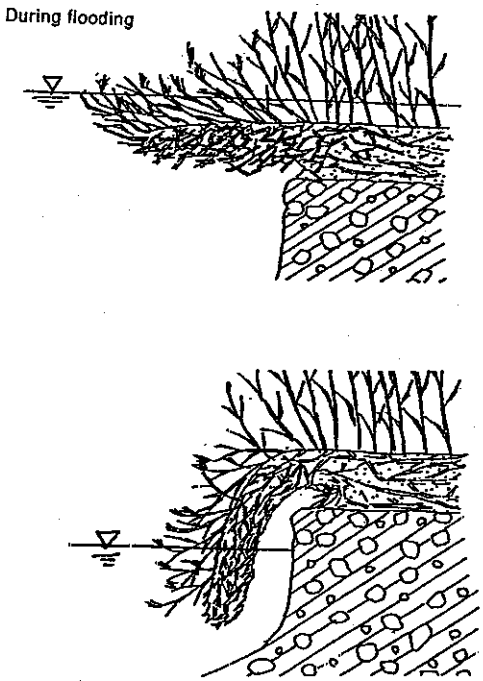

Figure 3: A bank with common reeds

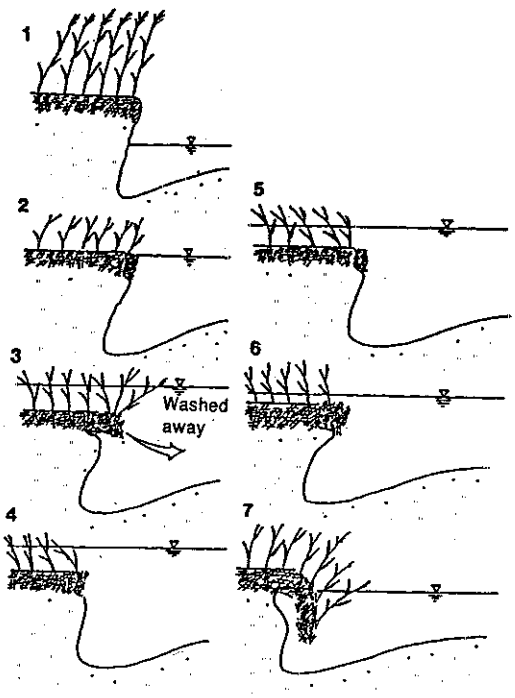

Figure 4: The erosion process in banks with reeds

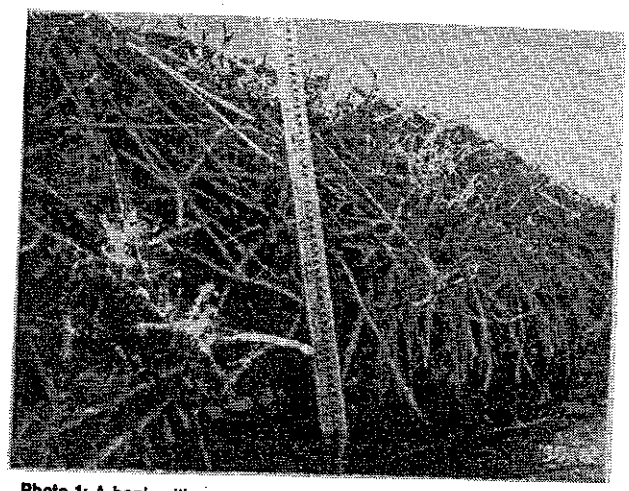

Photo 1: A bank with a protruding upper soil layer

Photo 1 shows this type of protruding layer of reed roots, often seen after flooding.

Let us now examine the process by which banks with common reeds are transformed into this protruding state more closely. Figure 4 shows the progression of bank erosion during flooding. When the water level rises, the lower layer of the bank is eroded as bed scouring occurs. Subterranean roots protect the upper layer, making it relatively resistant to erosion. As the sand around these subterranean roots, which are spread throughout the upper layer in a continuous mat-like form, is washed away, force is exerted on the network of subterranean roots, at which point, it is believed, the lower layer of the bank is then considerably eroded. Subterranean roots are centered around their nodes, and when fluid force is concentrated on these nodes, some experience tensile damage. Further erosion in the lower layer destroys the stability of the portion of the upper layer that contains reeds and soil, upon which the subterranean roots, unable to endure, suffer tensile damage, and bank erosion progresses. Further bank erosion occurs as this process is repeated. Although the buoyancy acting on the reeds keeps them afloat near the bank when the water level is high, both the reeds and the soil layer hang down when the flooding water level drops below the top of the flood channel. Velocity is still considerably high in this stage, but the upper layer which behaves like the *kinagashi-ko* (a method of flood fighting; see "Note") covers the banks and increases the roughness around the banks and, in addition to reducing velocity, attenuates the direct impact of water on the banks. During the waning phase of actual flooding in the Tama river, velocities of roughly 1.5 m/s were recorded with a water level roughly equivalent to the height of the flood channel

Note: *Kinagashi-ko*

A method of flood fighting for preventing a levee from being breached in which trees are cut at the root with branches and leaves intact, sandbags are placed on branches and trunks, and the bases are connected to the levee crown with iron wires with spikes in order to protect areas where flood water strikes.

2. The tensile strength of reeds and the critical velocity for the collapse of banks with a protruding upper soil layer [1) 3)]

During flooding, it is the nodes of subterranean roots of reeds that are destroyed. The reeds resist the force of the flow with the tensile strength of the nodes of their subterranean roots. The flexible structure of the nodes enables the reeds to change shape easily, and so the nodes of subterranean roots sustain tensile force in the direction that the above-ground stems do. It is therefore possible to estimate the erosion resistance of protruding upper layers by determining the tensile strength of the nodes.

To accurately measure the tensile strength of reeds, we measured it directly with an in-situ testing device developed for this purpose (see Photo 2). When tensile force is applied to the reeds, the roots gradually appear on the surface, and finally all nodes of the subterranean roots are torn out.

The measured results of maximum tensile force used as tensile strength are shown in Figure 5.

Photo 2: Tension testing device

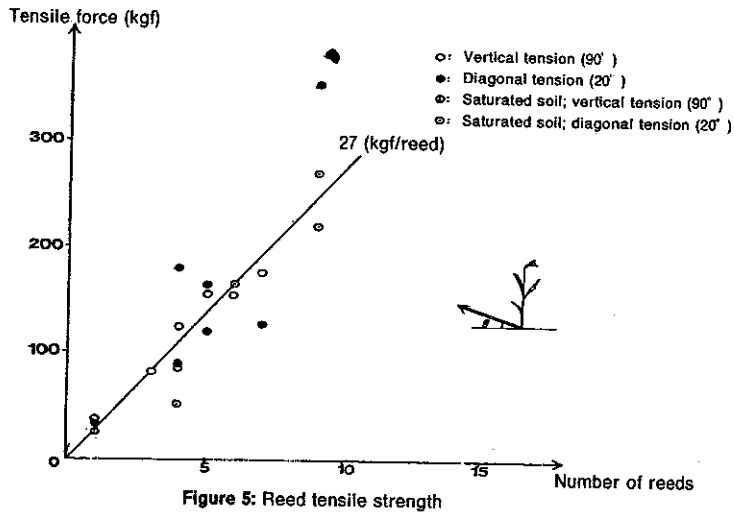

Figure 5: Reed tensile strength

While there is slight dispersion in tensile strength, Figure 5 shows that the tensile strength of a reed colony is roughly equivalent to the tensile strength of a single reed multiplied by the total number of reeds. Furthermore, this tensile strength can be assumed to be nearly constant regardless of the direction the reeds are pulled in and regardless of whether the surface is saturated or whether the reeds are near the bank or in a location in the flood channel far from the bank. The tensile strength per reed is 27 kgf on the average.

Determining the relationship between the length of protrusion and the critical velocity of protrusion collapse — i.e., the velocity at which the reeds can maintain the protrusion without collapsing — makes it possible to determine the location in the channel at which the reeds function to protect the bank. We shall therefore use the above-mentioned value of tensile strength of subterranean reed roots to determine the critical velocity of protrusion collapse.

Figure 6 shows the model of a bank protrusion with a certain size, which was used to estimate the critical velocity of protrusion collapse from the equilibrium between external force from the flow and the tensile force of the reeds' subterranean roots.

A protruding bank with a given height and width are subject to fluid forces. The bank is therefore submitted to the bending moment in xy plane and xz plane (Mxy and Mxz, respectively) because of fluid force F_x in the x-direction. Distribution of bending stress is produced by these bending moments, and so the stress in the y- and z-directions that acts on dB can be determined: As shown below, u_{cr} (the critical velocity of protrusion collapse) can be calculated from the equilibrium between F (the resultant force vector of the external force that acts on dB, the portion experiencing collapse) and R (the tensile strength of subterranean reed stems in the collapsed section), which equals $r\sigma' dB$.

$$u_{cr} = \left\{ \frac{2g \cdot r \cdot \sigma' \cdot dB}{\rho \cdot C_D \cdot L \cdot (K1^2 + L^2 \cdot K2^2 + K3^2)^{1/2}} \right\}^{1/2} \qquad \text{--------- (1)}$$

$$K1 = H + \varnothing \cdot h \cdot \sigma \cdot \int^{dB} f(x)^2 dx$$

$$K2 = 3L \cdot dB \cdot (1 - dB/b) \cdot (H + \varnothing \cdot h \cdot \sigma \cdot \int^{b} f(x)^2 dx) / b^2$$

$$K3 = 3 \cdot dB \cdot (1 - dB/b) \{ H^2 + \varnothing \cdot h \cdot \sigma \cdot (2H + h) \int^{b} f(x)^2 dx \} / b^2$$

where u_{cr} is the critical velocity of collapse; r, the tensile strength of subterranean reed stems (27 kgf/reed); σ', the number of subterranean reed stems per unit flow distance; f(x), exp (-2.15x); and b, the distance by which longitudinal velocity within reed colony u' subsides sufficiently (here, a value of b = 1m, the distance at which u' subsides by 90%, is used). Figure 7 shows a comparison of the calculated values of u_{cr} (critical velocity of collapse with L, the length of the protrusion, as the variable) and field data collected (near the 40-km point of the Tama river) following flooding. Here, the protrusion length recorded during post-flood surveying is used for L, while velocity measurements obtained during actual flooding are used for u.

The calculated values seem to provide a good explanation for the actual measured values, and Figure 7 contains no protrusion lengths (L) greater than 2 meters. This is because a difference of 2 meters of more between flood channel height and the water level in the main channel results in a protrusion length that collapses under their own weight, making it pointless to determine critical velocity.

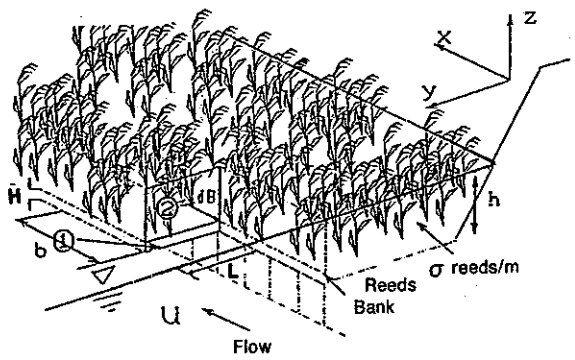

Figure 6: The flow model on bank with reeds

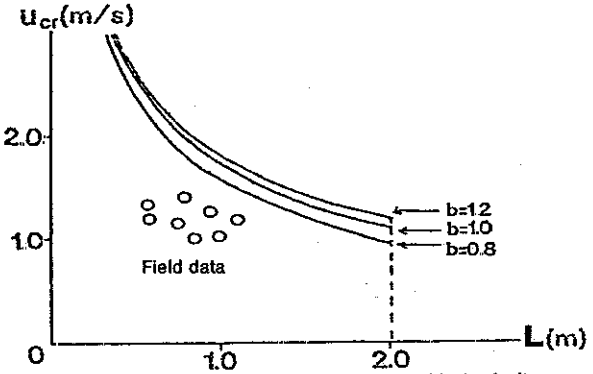

Figure 7: A comparison of field data and the critical velocity of protrusion collapse

3. How reeds attenuate the energy of waves produced by boats [4)]

Waves produced by passing boats are unpleasant to persons enjoying themselves on shore, and, as shown in Photo 3, can also cause significant bank erosion. However, if reeds growing at water's edge on the downstream portion of a river can attenuate the energy of waves produced by boats and preserve the calmness of the water surface while at the same time preventing bank erosion, it should be possible to utilize the flood-control and environmental functions of these reeds while also promoting their preservation and regeneration. A field survey was performed in the downstream portion of the Ara river in order to determine the extent to which reed colonies attenuate and reflect the energy produced by boats. This survey was performed on the right bank of the 14.5-km point of the Ara river. Two patrol boats were used: the Sumida and Arakawa, the specifications of which are shown in Figure 8.

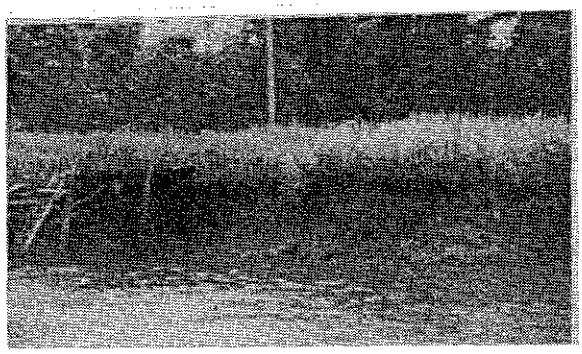

Photo 3: Bank erosion caused by boat waves

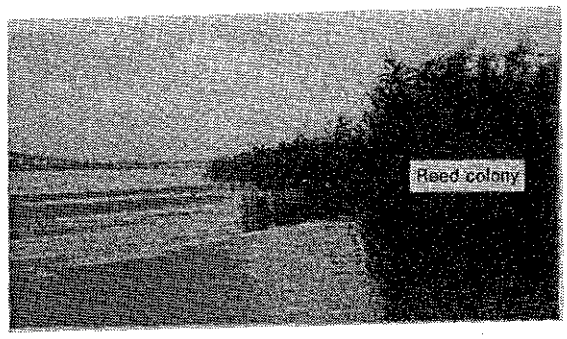

Photo 4: Waves produced by boats

The test area, being a tidal region, has an almost negligible current velocity. Depth was roughly 6 m at the point where the boats passed and 1.0 - 1.5 m in front of the reeds. Photo 3 shows the boat waves striking the reeds, and Table 1 shows the boat wave characteristics.

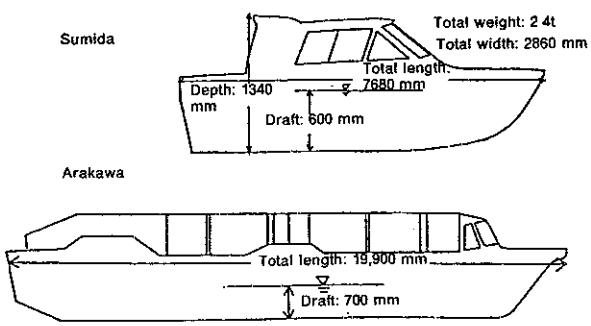

Figure 8: River patrol boats

Table 1: Characteristics of boat generated waves

	Sumida (patrol boat)	Arakawa (patrol boat)
Wave height	13 - 23 cm	6 - 52 cm
Wave celerity	1.85 - 2.67 m/s	2.11 - 3.56 m/s
Wave period	1.7 - 2.4 sec.	2.2 - 4.6 sec.
Wavelength	5.5 - 6.6 m	5.1 - 15.9 m
Number of waves	10 - 12	10 - 14

The energy conservation for the boat waves is expressed as follows.

$$W_I = W_T + W_R + W_L \text{ ---------- (2)}$$

where W_I, W_T and W_R respectively represent the energy transported per unit of width and unit of time by the incident waves, transmitted waves and reflected waves; W_L is the energy per unit of width and unit of time attenuated by the reeds; K_R (reflection coefficient) = H_R/H_I; K_T (transmissibility) = H_T/H_I; and the rate of energy loss is K_L. Thus, equation (2) is represented with the following equation.

$$1 = K_R^2 + K_T^2 + K_L \text{ ---------- (3)}$$

with which waves in the reeds are represented as being incompletely reflected and as having nodes and antinodes. After measuring the envelopes of the waves' crests and troughs, the value of K_R (reflection coefficient) was determined using Healy's method.

Figure 9, the relationship between the distance that the waves travel through the reeds and the rate of energy loss in the waves, shows that the rate of energy loss of a wave traveling 8 meters through the reeds approaches 60 to 80%. This allows us to conclude that the energy attenuation effect of the reeds is great even for large waves like those produced by the Arakawa patrol boat, and that the erosive force of waves on the bank beyond the reeds is almost zero. As shown in Figure 10, the wave reflection coefficient of the reeds is a mere 0.05 - 0.15, significantly smaller than the 0.2 - 0.35 reflection coefficient of tetrapods. This shows that reed colonies can quickly return the surface of the water to a state of calm following the passage of a boat, and hence are also effective in terms of river utilization.

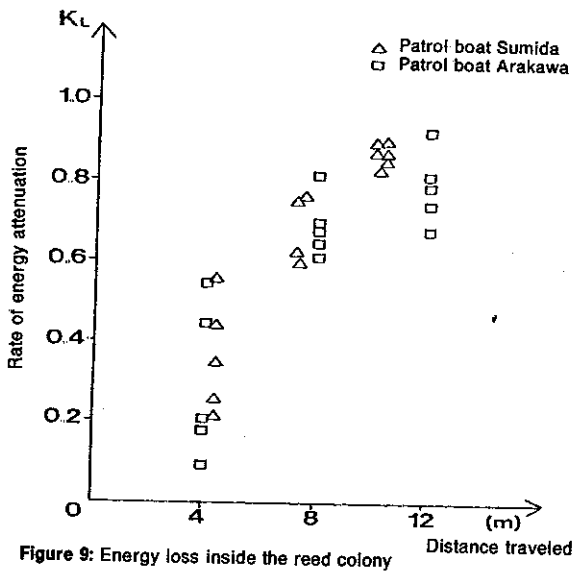

Figure 9: Energy loss inside the reed colony

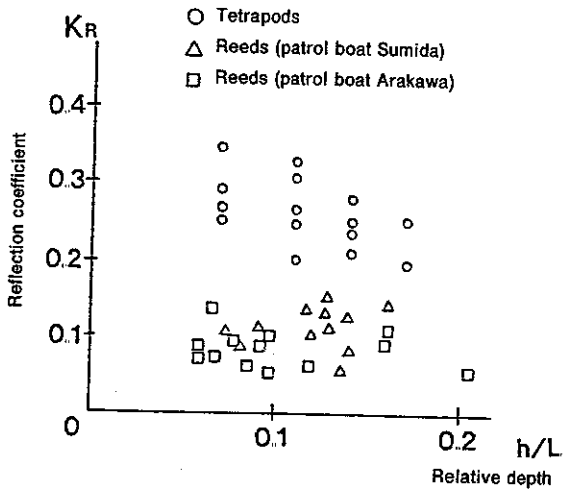

Figure 10: Reflection coefficient within the reed colony

The above reveals that the energy attenuation of reed colonies is sufficiently high in comparison with other artificial wave-reducing structures, while the calming effect and bank erosion attenuating effect of reed colonies also justifies their utilization in flood control and, in combination with their natural environmental functions, makes them capable of creating a safe and aesthetically pleasing aquatic environment.

4. The resistance of levee grass to current erosion [5)]

It is not yet clear to what extent grass on levees can resist the eroding action of currents. In order to estimate the erosion threshold of grass-covered levees and to use as basic reference data in levee design, as part of this research we performed erosion experiments on the surface of a flood channel covered with grass under certain hydraulic conditions, grass and soil properties.

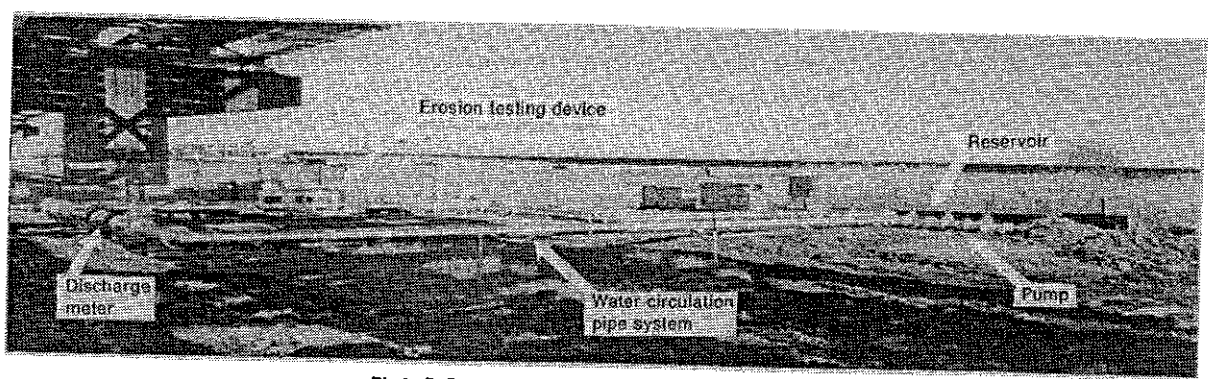

Photo 5: Overview of erosion experiment setup

This experiment was performed at three points on the flood channel near the 6-km point of the Tama river (see Photo 5). Table 2 shows the state of grass growth and the soil properties of the surface layer in which the grass is rooted. Also shown in the table is Edo river data used in this analysis [6) 8)]. The erosion testing device used was a 2-meter long, 0.12-meter high pipe conduit composed of an upper lid, body, and skirt board (see Figure 11). The skirt board was embedded directly in the grassy surface of the flood channel; the erosion depth, time, discharge and hydraulic gradient were measured as water flowed through.

Table 2: Soil characteristics at testing points

	Clay (%)	Silt (%)	Sand (%)	Gravel (%)	Grass coverage degree	Depth of root penetration (cm)	Thickness of root hair mat layer (cm)
Point a	6	23	71	0	5	30	5
Point b	16	30	50	4	3	20	5
Point c	21	38	28	13	4	15	5
Edo river	22	61	17	0	4	3	3

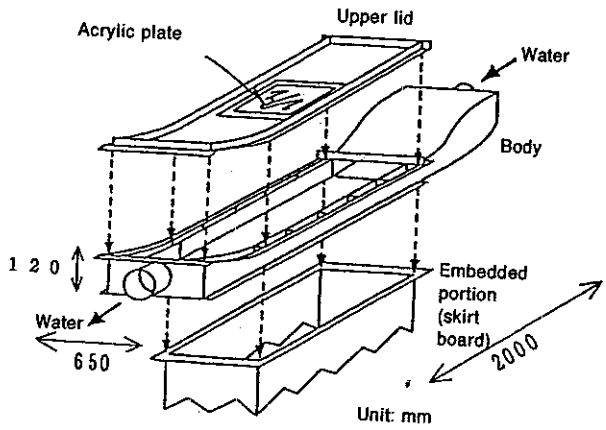

Figure 11: Erosion testing device

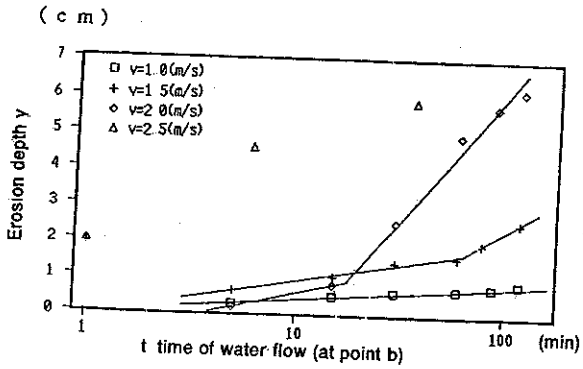

Figure 12: Changes over time in erosion depth

In the erosion process, first soil in the surface layer is carried away, after which erosion gradually progresses to the root hair mat layer. Eventually the grass is partially torn away, then, finally, completely torn away. As the stages up to which the entire root network of the grass is destroyed are the stages in which the grass possesses erosion resistance, these stages make the subject of the experiment. The measured results of a typical case are shown in Figure 12. When these measured results are plotted with y (mean erosion depth) as the vertical axis and the logarithm of t (time of water flow) as the horizontal axis, erosion depth can be expressed as $y = A \log t$. The rapid increase in erosion depth in the graph when v = 2 m/s indicates that this is when the root network of the grass was destroyed. Figure 13 shows the relationship between the value of A and the bed shearing stress (τ_b), which was determined using the measured hydraulic gradient. This graph shows that the value of A and friction velocity $\sqrt{\tau_b/\rho}$ are roughly proportional, which allows us to express mean erosion depth thus: $y = \alpha\sqrt{\tau_b/\rho} \log t$, where α is a parameter relevant to soil and grass characteristics.

Because the complex relationship of grass erosion depth with soil and grass properties makes a derivation of a theoretical solution difficult, a dimensional analysis method is used here. Physical quantities related to mean erosion depth include bed shearing stress (τ_b), time (t), maximum root length (R_{max}), soil particle cohesion (c), the fine particle component (F) and grass coverage degree (H). Here, "coverage degree" refers to the percentage of the surface area in question covered by grass. [7)] Dimensional analysis is used to express erosion depth with the following equation.

$$\frac{y}{R_{max}} = f\left(\frac{\tau_b}{c}, \frac{\tau_b}{\rho}\cdot\frac{t}{R_{max}}, F, H\right) \quad \text{---------- (4)}$$

Upon comparing and contrasting the above equation with the equation obtained through experimentation ($y = \alpha\sqrt{\tau_b/\rho} \log t$), it becomes possible to relate α to C, F, R_{max} and H.

Using measured results and this dimensional analysis, let us consider parameter α. Figure 14 shows the relationship of α with the fine particle component of the soil, grass coverage degree and root depth as determined in this experiment and a separate experiment performed by Fukuoka and Fujita. [6) 8)] According to this experiment and a separate survey on levee soil and levee grass in the Tama river, at least 50% of the levee surface soil through which the root network had spread was fine particles of clay and silt; the grass coverage degree was 4 and the root depth was an average of 20 cm. This shows that soil and grass properties are nearly similar to those at the Edo river and at points b and c. Figure 14 also shows that the relationship between α and the fine particle component at these three points can be approximated with a straight line as

$$\alpha = -0.18F + 14.5, \text{ at } F > 40\% \quad \text{----------(5)}$$

In addition, point a has high erosion resistance because of the large sand component and the resulting deep roots and dense growths of grass. This point has been excluded from these calculations because it has surface soil qualities different from those of typical levees.

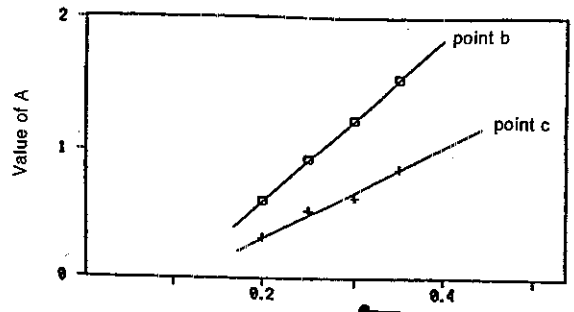

Figure 13: The relationship between A and friction velocity

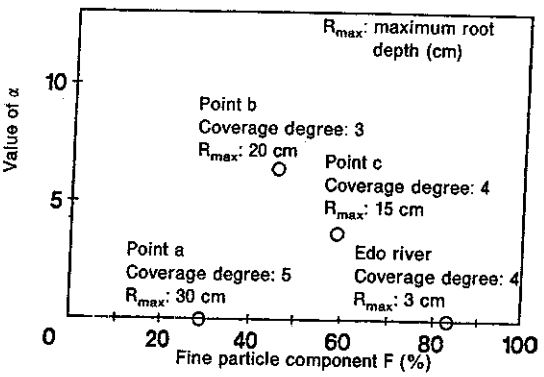

Figure 14: Relationship between α and F

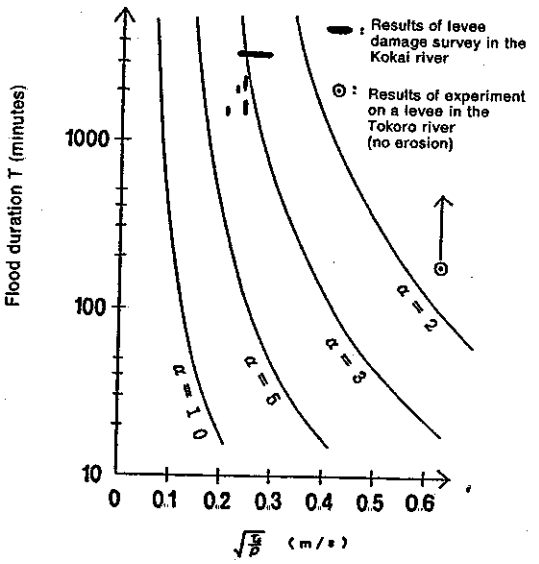

Figure 15: Erosion threshold diagram

As the value of α can be roughly estimated from the value of F, the previous equation is used to determine the relationship between submersion time and bed shearing stress at the time when the levee protecting effect of the grass' roots is lost. Also, the threshold erosion depth, set at half the thickness of the root hair mat layer, is estimated with a margin for safety. This relationship when α is the parameter is shown in Figure 15. The grass is torn away at the upper right of these curves, at which time erosion occurs. Upon plotting in Figure 15 the results of a levee damage survey performed in the Kokai river by the Public Works Research Institute,[6] the points were concentrated to the right of a curve representing α = 5. It shows that soil of the Kokai river levee has a fine particle component of roughly 60%, a grass coverage degree of 4 and root depth of roughly 15 cm. Applying Figure 14 with these conditions, α has a value of roughly 5, showing that Figure 15 has produced fairly accurate results for the erosion threshold of actual rivers.

5. Predicting water levels during flooding in rivers with vegetation and the use of vegetation in river plan and management [2) 10)]

Hydraulically, a river vegetation is a large roughness element and is an important element in developing a river close to its natural state. Hence, we must consider solutions and countermeasures to the following problems in order to handle river vegetation in planning and management.

Taking account of such factors as channel cross-sectional area and levee alignment, we must determine the location and range of vegetation that should be conserved or cleared in order to prevent the vegetation from reducing the channel's discharge capacity and to avoid any negative effects on the levee. Also, for levee protection, river utilization and ecosystem preservation, it is necessary to determine the range of vegetation to be conserved as well as locations on flood channels where such vegetation can be grown. To this end, high-accuracy calculation methods for determining water levels during flooding in channels with vegetation are indispensable.

Our goal is to calculate, as resistance forces, the effects of vegetation on flows and to establish a practical and high-accuracy method for predicting water levels in channels with vegetation. Specifically, as shown in Figure 16, we assume a section from which the dead-water region produced by vegetation is excluded and in which the vegetation height is designated as the ground level. Cross-sectional profiles determined in this manner are similar to the cross-sectional profiles of compound channels.[9] Next, assuming that shearing stresses τ and τ' act on the vegetation boundary as well as the boundary between the main channel and flood channel, an equation for depth-averaged lateral velocity distribution in a given section is derived that is capable of expressing flow acceleration and deceleration caused by the vegetation.

The continuity equation and equation of motion for each divided section can be expressed with equations (6) and (7), shown below.

$$\frac{n_i^2 u_i^2}{R_i^{4/3}} S_{bi} + \frac{\Sigma(\tau'_j S'_{wj})}{\rho g} + \frac{\Sigma(\tau_j S_{wj})}{\rho g} = A_i I_b \quad \text{---------(6)}$$

$$Q = \Sigma(A_i u_i) \quad \text{---------(7)}$$

where u_i is the average velocity for a divided section; n_i, R_i and A_i are the roughness coefficient, hydraulic radius and cross-sectional area (from which the dead-water region has been excluded), respectively, for each divided section; S_{bi} is the length of the wetted perimeter on which the shearing stress of the side wall acts; τ_j and τ'_j are the shearing stresses acting on the vegetation boundary and divided section boundary, respectively; S_{wj} and S'_{wj} are the lengths of the wetted perimeters on which τ_j and τ'_j act; and I_b is the bed slope. The leftmost term is the shearing stress acting on the side wall; the second term from the left is the shearing stress that acts on the boundary of each divided section; the

third term from the left is the shearing stress that acts on the vegetation boundary; while the rightmost term is the downstream component of gravity

Using the lateral velocity distribution determined with these calculations, the shearing stresses acting on the side wall and vegetation boundary are calculated. Then, in accordance with the principle of momentum, an equation for calculating the longitudinal water-level changes in a channel with vegetation is derived.

$$\frac{\partial}{\partial x}\left\{\frac{1}{A}\left(\Sigma\frac{u_i^2 A_i}{2g}\right)+H\right\}=\frac{1}{A}\Sigma\left(\frac{n_i^2 u_i^2}{R_i^{4/3}}S_{bi}\right)+\frac{1}{\rho g A}\Sigma\left(\tau_i S_{vi}\right) \quad \text{---------} \quad (8)$$

where H is the water level; H = z + h; A is ΣA_i; the rightmost term is the average value in a section of the shearing stress acting on the side wall; and the second term from the right is the average value in a section of the shearing stress acting on the vegetation boundary. Also, the depth averaged lateral velocity distribution calculated with equations (6) and (7) is assigned to u_i in equation (8).

Figure 17 and 18 — the results of the application of this equation on the Ishikari river — show that the calculated values for lateral velocity distribution and water level during flooding for a channel with various types of dense vegetation accurately reflect actual measurements. This method has hence provided us with a valuable method of technical examination in utilizing the above-mentioned vegetation in flood-control measures.

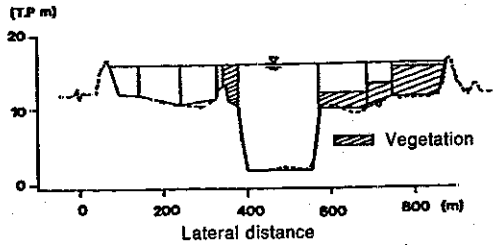

Figure 16: The section used in these calculations

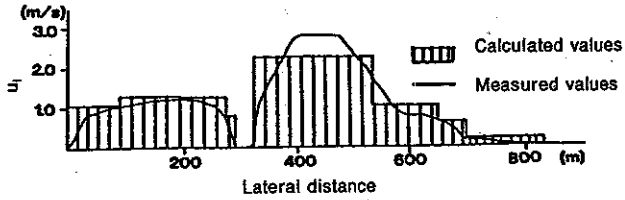

Figure 17: The calculated depth averaged lateral velocity distribution

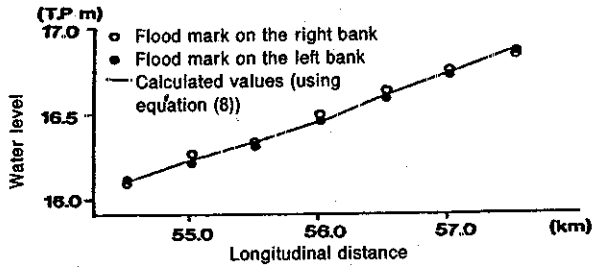

Figure 18: The calculated longitudinal water level

Conclusion

In this paper we have discussed new river-related techniques for utilizing channel vegetation as part of flood-control measures, and it would seem appropriate to proceed with diversified river projects through actual field application with technical assessment combined with a broad approach to river functions.

References

1) FUKUOKA, Shoji: Bank Erosion and Natural Bank Protection, Proc. of Symposium of Sediment Transport Phenomena, pp. 83-114, 1992. (in Japanese)

2) FUKUOKA, Shoji and Koh-ichi FUJITA: Hydraulic Effects of Luxuriant Vegetations on Flood Flow, Report of Public Works Research Institute, pp. 129-192, 1990. (in Japanese).

3) FUKUOKA, Shoji, Hiroshi NI-IDA and Kenji SATO: Control Mechanism and Resistant Strength of Common Reeds against River Bank Erosion, Proc. of Hydraulic Engineering, JSCE, Vol. 36, pp. 81-86, 1992. (in Japanese).

4) FUKUOKA, Shoji, Kenyu KOMURA and Akihide WATANABE: Effect of Marsh Reeds in the River on the Energy Dissipation of Boat-Generated Waves, Proc. of Hydraulic Engineering, JSCE, Vol. 36, pp. 713-716, 1992. (in Japanese).

5) KAKINUMA, Takaharu, Shoji FUKUOKA and Yorinori EBATA: Erosion Resistance of the Grass-covered Soils by the Flowing Water, Annual Conference on Civil Engineering, Vol. II, No. 48, 1993. (in Japanese).

6) FUKUOKA, Shoji and Koh-ichi FUJITA: Erosion Resisting Characteristics of Grass-Covered Levee, Civil Engineering Journal, Vol. 29, No. 12, pp. 44-49, 1987. (in Japanese)

7) Ministry of Construction: Technical Criteria for River Works, Sankaido, 1997. (in Japanese)

8) FUKUOKA, Shoji and Koh-ichi FUJITA: Erosion Limit of Sod on the Slope of Levee; Proc. of Hydraulic Engineering, JSCE, Vol. 34, pp. 319-324, 1990 (in Japanese)

9) FUKUOKA Shoji and Koh-ichi FUJITA: Prediction Method of Flow Resistance in Rivers with Compound Channels and Application to River Course Design, Int. Conference on River Flood Hydraulics, pp. 113-122, Wiley, 1990.

10) FUKUOKA, Shoji and Koh-ichi FUJITA: Water Level Prediction in River Courses with Vegetation, Proc. of XXV IAHR Congress, Tokyo, 1993, Prediction in Flood Water Level of River Courses with Vegetation, Proc. JSCE, No. 447/II-19, pp. 17-24, 1992. (in Japanese).